Proceedings of ASME Turbo Expo 2024
Turbomachinery Technical Conference and Exposition
GT2024
June 24-28, 2024, London, United Kingdom

GT2024-128732

EXPERIMENTAL STUDY ON STABILITY ENHANCEMENT OF A NATURAL GAS GT BURNER WITH HYDROGEN FLAME PILOTING OPERATED WITH SIMULATED EXHAUST GAS RECIRCULATION

S. Galeotti*[1], A. Picchi[1], R. Becchi[1], G. Lemmi[1], R. Meloni[2], G. Babazzi[2], N. Giannini[2] ,B. Facchini[1],A. Andreini[1]
[1]DIEF - Department of Industrial Engineering of Florence - University of Florence - Via S. Marta 3, 50139, Florence, Italy
[2]Baker Hughes - Via Felice Matteucci 2, 50127, Florence, Italy
*sofia.galeotti@unifi.it

ABSTRACT

Efficient coupling between gas turbine power plants fuelled with natural gas and Carbon Capture and Storage (CCS) units can be achieved by taking advantage of turbine Exhaust Gas Recirculation (EGR), since CCS efficiency increases with the CO_2 content of the incoming flow. On the other hand, the combustion process has to endure the reduction of overall flame reactivity caused by EGR, with a potential increase of CO and UHC emissions, and modifications in the flame dynamic behaviour. In order to extend the combustor operability window, non-conventional pilot flames can be exploited to improve overall flame stabilization: in the current study the use of local hydrogen pilots was investigated. A lean-premixed burner for heavy-duty Gas Turbines was studied at ambient pressure in a reactive single-cup test rig at the THT Lab of the University of Florence, replicating EGR with the addition of CO_2 to the combustion air. Reactive PIV measurements revealed a jet flame flowfield, not significantly affected by simulated EGR, which instead alters substantially the flame structure. Hydrogen addition has been found beneficial in widening the burner operating window, allowing higher premix splits to be achieved and reducing pressure oscillations also in EGR conditions. A modest decrease in CO emissions with high EGR levels was observed, and the flame structure detected with OH chemiluminescence suggests that an optimization of the pilot injection geometry for dual fuel configuration could remarkably improve burner performance with EGR by enhancing the interaction between hydrogen pilot jets and natural gas flame.*

NOMENCLATURE

Acronyms

BH	Baker Hughes
CCS	Carbon Capture and Storage
DLN	Dry Low NO_x
EGR	Exhaust Gas Recirculation
FoV	Field of View
GT	Gas Turbine
LBO	Lean Blow Out
NG	Natural Gas
PIV	Particle Image Velocimetry
RMS	Root Mean Square
UHC	Unburned Hydro-Carbon

Symbols

CO_2%	CO_2 dilution rate	[%]
CS	Combustor oxidizer mass flow split	[-]
$\Delta P/P$	Combustor pressure drop	[%]
D	Burner outlet diameter	[mm]
EGR%	Exhaust Gas Recirculation rate	[%]
ERT	Extinction Residence Time	[s]
ESR	Extinction Strain Rate	[1/s]
m	Mass flow rate	[kg/s]
PMX%	Premix fuel thermal power fraction	[%]

PLT%	Pilot fuel thermal power fraction	[%]
P'_{RMS}	RMS of pressure oscillation	[mbar]
REF	Reference Value	
S_d	Laminar Flame speed	[m/s]
T_{flame}	Adiabatic flame temperature	[-]
T_{inlet}	Inlet temperature	[°C]
TP	Thermal power	[kW]
TP(H_2) %	Hydrogen thermal power fraction	[%]
U	Axial velocity	[m/s]
V	Radial velocity	[m/s]
UV	Velocity magnitude on xy plane	[m/s]
x	Axial coordinate	[mm]
y	Radial coordinate	[mm]
y_{O2}	Inlet oxygen mass fraction	[%mass]
λ	Wavelength	[nm]

INTRODUCTION

As the world focuses on meeting climate goals and minimizing the impact of greenhouse gas emissions, demand is growing for efficient methods to mitigate the negative effects of carbon dioxide (CO_2). Despite the rise of renewable energy sources, the use of natural gas in the energy sector is expected to grow due to its versatility [1]. To aid in emission reduction efforts, innovative technologies such as Carbon Capture and Storage (CCS) systems integrated with gas turbine power plants could become an interesting option.

CCS systems' efficiency improves as the CO_2 concentration in turbine exhaust increases, a factor that can be enhanced through Exhaust Gas Recirculation (EGR) [2, 3]. EGR, a well-established method in internal combustion engines to limit NO_x emissions by reducing the flame temperature, hasn't been widely applied in Gas Turbine engines due to high costs and complexity in installation, with NO_x reduction comparable with modern Dry Low NO_x (DLN) combustion technologies [4]. Nevertheless, EGR presents an attractive option for Gas Turbines by potentially enhancing the coupling with CCS units through increased CO_2 content in exhaust gases. Furthermore, EGR is found to be beneficial for NO_x reduction under gas turbine conditions [5, 6]. Yet, challenges arise from decreased oxygen content, posing difficulties for combustion stability. Investigations on thermodynamics and kinetics effect of CO_2 enrichment on the laminar flame speed, both experimental and numerical, revealed that the change in the oxidizer composition strongly affects the reactivity [7–9], and CO_2 is not an inert from the kinetics point of view [10].

Past investigations into EGR's impact at engine conditions revealed a notable increase in CO and UHC emissions, limiting achievable EGR levels [5, 11–13]. While [5] suggests positive effects on damping thermoacoustic instabilities, recent works confirm the rise in CO emissions with EGR [14], though its impact on flame dynamics is not univocal. Notably, recent research indicates that at extremely low oxygen levels not only the lack of oxygen but also the chemical composition of the oxidizer can influence the dynamic flame response [15].

In order to help the flame stabilization in these challenging conditions, injection of localized hydrogen pilots could be exploited, because of hydrogen enhanced reactivity.

The impact of a small addition of hydrogen on NO_x in methane-air flame has been investigated for classic DLN systems [16]. Anderson et al. [17] in one of the earliest studies noted that in a perforated-plate flame holder configuration hydrogen injection would stabilize the flame and make it quieter. More recently Oztarlik et al. [18] proved that the injection of small hydrogen amount is able to stabilize a thermo-acoustically unstable flame, but with a negative impact on NO_x levels. Similar results were found also by Barbosa et al. [19] for a lean propane-air premixed flame, with reduced oscillations with swirled hydrogen injection, with limited NO_x emissions but with a significant increase in CO.

The present work has the purpose of contributing to the development of new burner concepts, able to efficiently operate in unconventional operating conditions such as exhaust gas recirculation. In particular the effect of hydrogen pilot flames in a natural gas fuelled industrial burner has been studied in the present work. This investigation represents the second step of a more extended experimental campaign, following the characterization of the baseline burner presented in [20], where tests have been performed in a tubular sector rig at ambient pressure in conditions that simulate the lack of oxygen caused by EGR, with natural gas as fuel. As for the present work EGR conditions were replicated by vitiating the combustion air with CO_2 to lower the oxygen content. The change in the flame structure with the inlet oxygen level and the fuel split between premix and pilot lines has been investigated with OH* chemiluminescence, showing that the reaction zone becomes widespread and less intense as the oxygen level in the oxidizer decreases. NO_x emissions were significantly lowered with simulated EGR, but CO levels on the other hand, as expected increased greatly, more than 10 times the value without EGR. Thermoacoustic instabilities were found to be triggered by the variation in the oxidizer composition, with increasing amplitude with higher premixing level, up to a threshold on the inlet oxygen level, under which pressure oscillation decreased.

For the present work, the same burner has been tested in similar conditions with hydrogen addition on the pilot fuel line, with the purpose of enhancing flame stability. Tests at ambient pressure have been performed, varying the inlet oxygen level, the thermal power split between pilot and premixed lines and the hydrogen content. Experimental results are divided into three sections, starting with the extension of the characterization of the burner fed with natural gas, with 2D PIV velocity field measurements and OH* chemiluminescence, followed by the study of the effects of hydrogen addition first with standard air

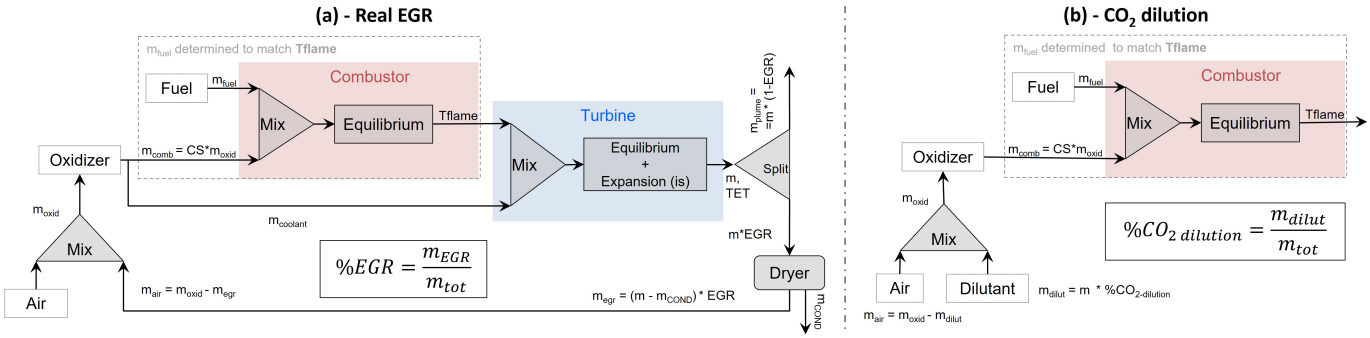

Figure 1: Cantera function schemes for calculating the reactants composition for real dry EGR (a) or CO_2 dilution (b)

as oxidizer, and finally with simulated EGR, in terms of flame topology, emissions and dynamic behaviour.

As anticipated EGR conditions have been simulated with the addition of CO_2 in the combustion air, which is significantly more convenient in terms of experimental test management than mixture with nitrogen or even real recirculation of the exhaust. A dedicated numerical study with chemical kinetics tools has been performed, to verify that the purpose of the investigation is retained and CO_2 dilution is substantially able to reproduce EGR conditions.

This and the previous test campaign are part of the European project TRANSITION (fuTure hydRogen Assisted gas turbiNeS for effective carbon capTure IntegratiON) which has the purpose of developing advanced combustion technologies for natural gas fired gas turbines to permit engine operations with high EGR rates, with a consequent drastic reduction of the CCS costs and units' size [21]. Experimental tests with a single sector test rig at ambient pressure can be considered the first step of a design improvement to be placed inside the more general project work frame.

CHEMICAL KINETICS PRELIMINARY STUDY

As previously mentioned, from the experimental standpoint the effect of the EGR is simulated through a CO_2 dilution of the oxidizer. While this approximation significantly simplifies the experimental setup, it necessitates careful consideration and discussion. A comparative analysis between real (dry) EGR and CO_2 vitiated conditions was performed with Cantera (library 2.5.1 [22] in Python 3.9.12 environment), aimed at gaining a general understanding of the impact on the thermo-kinetics of the combustion process. In particular, the key parameters chosen for the study are the Laminar Flame Speed (S_d), the extinction strain rate (ESR) and blow-out limits (LBO), which have been considered crucial, since the primary effect of EGR is an overall reduction of reactivity.

Figure 1 depicts the function framework employed for the analysis: (a) is the scheme of dry EGR implemented on a real gas turbine, while (b) represents the experimental test rig, with CO_2 dilution. Starting with the real EGR, the composition of the mixture entering the combustion chamber depends on the recirculating products, which are, in turn, the outcome of the combustion of an unknown mixture composition, and therefore solving this problem demands an iterative approach. Additionally, gas turbines have a certain dilution rate between the air entering the combustion chamber and the turbine exhaust: combustion split (CS) is defined as the ratio between the oxidizer mass flow rate entering the combustor and the total oxidizer mass flow rate, which includes cooling air for the combustor and early turbine stages, and other secondary flows. The value is highly dependent on the turbine class and, in the case of variable/adaptive geometry, also on the operating conditions. The reaction process is simulated by bringing to equilibrium fuel and the combustor fraction of oxidizer. Subsequently, products are mixed with the oxidizer portion that didn't take part in the reaction and brought to equilibrium conditions through the introduction of an isoentropic expansion, simulating the flow thermodynamic behaviour within the turbine. Most of the water content of the exhaust is then removed with the dryer, which considers a vapor saturation temperature of 5°C, and finally the loop is closed with the dried exhaust recirculated and mixed with fresh air.

The CO_2 dilution layout is much simpler, since there is no need for the iterative approach and mixture composition is defined a-priori with the concentration of each chemical species.

The two operating schemes shown in Figure 1 have been used to define the composition of the mixture entering the combustion chamber, as a function of the two control parameters, which are %EGR and $\%CO_2$, defined respectively with the recirculated or CO_2 mass flow rates over the total one, as reported in the diagrams. The results are reported in Figure 2 in terms of oxygen mass fraction as a function of the adiabatic flame temperature and the EGR level or the CO_2 dilution. For the CO_2 dilution map, the curves at equal T_{flame} are not horizontal only

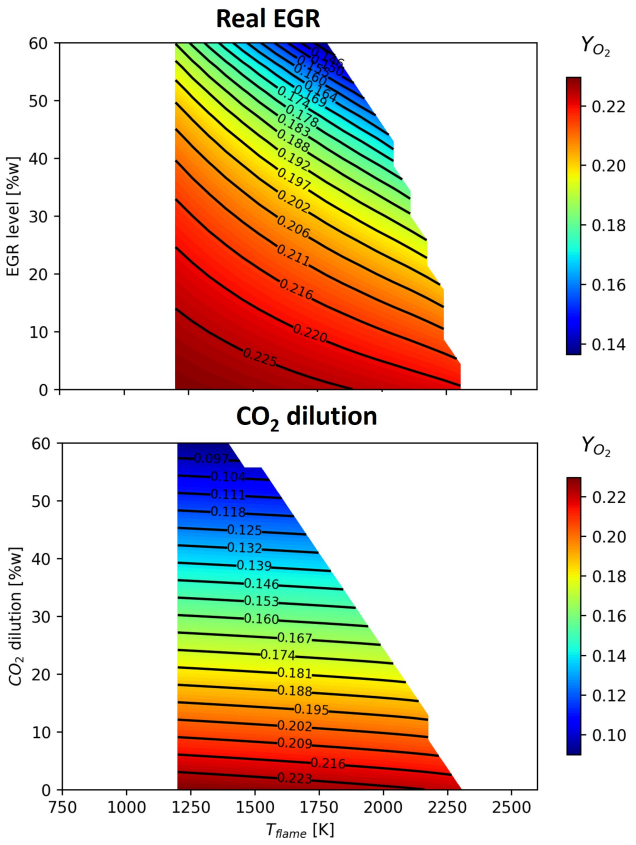

Figure 2: Contour maps of the oxygen mass fraction within the fresh mixture as a function of the adiabatic flame temperature and the EGR level or the CO_2 dilution

because of thermal effects, as the change in product composition affects the average specific heat.

The matching between experimental conditions with CO_2 dilution and real EGR, is made by targeting both adiabatic flame temperature and oxygen inlet concentration. In order to assess the differences between these two approaches, the effect on the laminar flame speed due to the different oxidizer composition has been evaluated. A freely propagating 1D premixed flame from the FreeFlame class in Cantera has been solved, with the mixture composition of Figure 2 for both scenarios. The resulting laminar flame speed for a fixed T_{flame} is reported in Figure 3a as a function of the inlet oxygen mass fraction. With CO_2 dilution laminar flame speed is slightly lower, with increasing difference with respect to real EGR as the inlet oxygen content decreases, i.e. EGR level increases. Comparison of real EGR and CO_2 dilution has been also performed in terms of blow-out occurrence and strain resistance. As before, the analysis has been carried out by targeting both the same adiabatic flame temperature and inlet oxygen mass fraction concentration for the two cases. For the blow-out study, a constant volume Perfectly Stirred Reactor (PSR) was considered with the same operating conditions as the experimental test rig, therefore ambient pressure and natural gas as fuel, and the detailed GRI 3.0 was used as reaction mechanism. The PSR is initially filled with equilibrium products to simulate ignition, followed by a progressive residence time reduction until blow-out is reached. The effects on the extinction strain rate of both EGR and CO_2 dilution, on the other hand, are evaluated by computing the highest strain rate value at which a counter-flow diffusion flame can be sustained before it undergoes extinction. The results of these analyses are reported in Figure 3b and c for the extinction residence time and extinction strain rate respectively. As expected, the extinction residence time rises as the oxygen mass fraction decreases, which corresponds to higher levels of EGR or CO_2 dilution. The steeper slope of the CO_2 dilution CO_2 indicates a higher vulnerability to blow-out in contrast to real EGR conditions. Similar observations can be made for the ESR analysis, with CO_2 dilution facing flame extinction for lower values of the strain rate, thus indicating a reduced combustion stability compared to real EGR, with increasing difference as the oxygen mass fraction decreases.

The presented results show that CO_2 dilution creates more challenging conditions for flame stability compared to real Exhaust Gas Recirculation (EGR). The choice of using CO_2 dilution for conducting experimental tests, while not rigorous, can be considered a conservative and precautionary approach. This underscores the validity of this approximation as a precautionary and robust experimental method, in the perspective of a general preliminary screening, considering different burners and various solutions to improve flame stability, all compared under the same conditions.

The comparison of real EGR with CO_2 dilution in terms of chemical reactivity has been performed only with natural gas as fuel, since it was intended to be a more general study of this topic. Additionally, numerical tools have also been employed to estimate an upper limit on the fraction of hydrogen that can be used to improve flame stability. In fact, it has to be kept in mind that the primary goal is to increase CO_2 concentration at the exhaust, and of course the use of hydrogen goes in the opposite direction. In this sense a maximum value of 10% of the total thermal power has been estimated as a good trade-off between higher achievable EGR and a limited reduction of CO_2 at the exhaust. In particular, it has been estimated with the Cantera framework reported in Figure 1, that with 10% of hydrogen on the total thermal power, it is necessary to increase the EGR level by 6% to achieve the same CO_2 concentration at the exhaust, which has been considered a reasonable compromise.

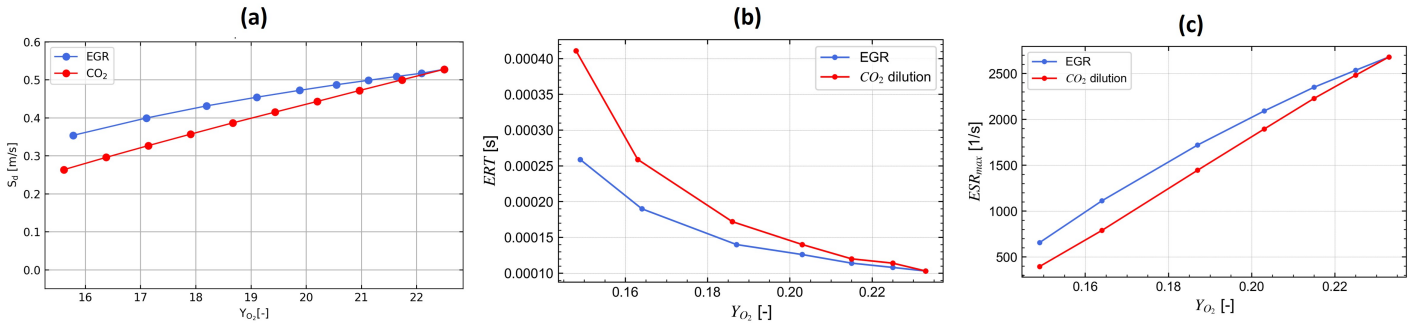

Figure 3: Comparison of Laminar Flame Speed (a) Extinction Residence Time (b) and Extinction Strain Rate (c) for real EGR and CO_2 dilution

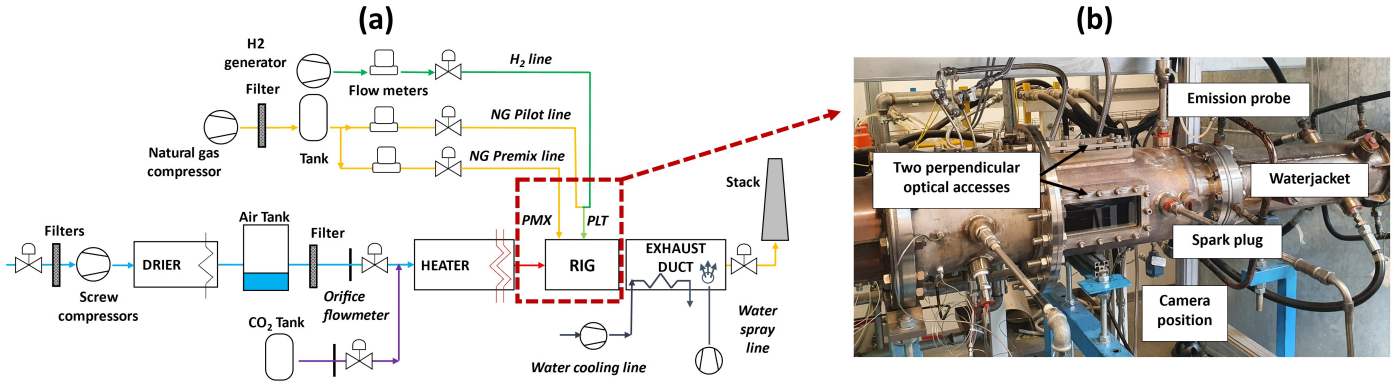

Figure 4: Combustion test cell plant (a) and picture of the reactive test rig (b) at the THT Lab of the University of Florence

INVESTIGATED BURNER AND TEST RIG

Test rig configuration

The experimental campaign has been conducted at the THT Lab of the University of Florence. Figure 4a reports a schematic of the layout of the reactive test cell, which has been used in the past for investigations on novel low NO_x burners for heavy-duty gas turbines [23, 24]. Two screw compressors deliver up to 1 kg/s at 10 barA of compressed air, which flows through several filters and a dryer (dew point -20°C) before entering into the test cell. An electric heater (up to 600kW) is used to increase the temperature of the air entering the test cell, with power input controlled with a proportional integral derivative system. A globe valve upstream of the heater is used to control the air mass flow rate, which is measured with calibrated orifice flow-meters (standard EN ISO 5167-1), with an error of 1% according to the Kline and McClintock method [25]. A water jacket exhaust duct with straight circular cross section (about 1 m length) is installed downstream of the test section. It is equipped with four water sprayers, used to quench the exhaust before the stack.

As explained in the introduction, and supported by the chemical kinetic study presented in the previous section, CO_2 addition in the airflow feeding the burner has been employed to reproduce EGR condition, since it offers the opportunity to manage storage better than mixtures with nitrogen, while preserving the purpose of the investigation. CO_2 is injected upstream the electric heater, in order to deliver a homogeneous mixture in terms of temperature and composition to the test section.

Regarding the fuel lines, hydrogen is not stored and only produced on demand with an electrolizer, which can deliver up to 14000 Nlt/h of hydrogen at 8 bar, with a purity of 99.5 ± 0,2%.

Natural gas is taken from the local gas network (20 mbar) and compressed to 16 bar. Since natural gas exact composition can vary throughout the day, it is analyzed after each test. In order to smooth out pressure fluctuations a 200 liters tank is installed on the delivery line. Fuel mass flow rates are controlled with globe valves and measured with orifice flow meters. Shut-off valves are also installed along the lines for safety reasons.

A picture of the reactive test rig is shown in Figure 4b, and the cross-section of the test article is reported in Figure 5a. The same test rig has been employed in a similar test campaign with a

different BH burner, described thoroughly in [26], together with additional details on the test rig.

The test rig is composed by an external casing, consisting of an upstream and downstream vessel, and an inner test section. The burner is installed on the upstream vessel with a special flange designed to accommodate BH burners from real engines without the need for modifications. The outer downstream vessel is equipped with two perpendicular quartz windows, required for PIV measurements for image acquisition and laser sheet entrance. The combustion chamber is made of a 2.5 mm thick cylindrical quartz cylinder, about 2.5 diameters long, and a downstream metal duct used to convey the exhaust gases to the test rig exhaust system. The liner outer walls are cooled by forced convection of a fraction of the incoming air that flows in the annulus between the liner and the confining vessel, not used in the combustion process. The dome plate is equipped with effusion cooling holes, and cooling air from the dome enters the combustion chamber, along with air flowing inside two swirlers of the burner. Dedicated flow checks were performed to evaluate the effusion holes effective area to evaluate precisely the airflow inside the combustion chamber. A spark plug is used for ignition, and it is located along the flame tube downstream of the optical liner.

Burner description

The burner investigated in this work is the baseline configuration selected for the study on EGR, a well established design employed by Baker Hughes for industrial gas turbine applications. It is a lean premixed burner, derived from an aero-derivative design, whose main characteristic is the versatility to operate stably under widely varying conditions [27]. A thorough description of the burner, with improved performances for low NO_x emissions can be found in [28–30].

A schematic of the burner cross section is reported in Figure 5b. It is composed of two counter-rotating axial swirlers, a center body and a converging nozzle. For the investigated configuration two independent fuel lines are present: the premixed line (PMX) delivers the fuel at the tip of the inner swirler in a jet cross flow configuration. Strong mixing is ensured thanks to the intense turbulence created by the shear layer generated between the two swirler in the converging nozzle, which follows the swirler before entering the combustion chamber [31]. The pilot line (PLT) injects the fuel directly into the combustor chamber through circumferentially equally spaced holes, helping the flame stabilization and allowing safe and stable natural gas operation with different engine loads, keeping an adequate margin for NO_x emission requirements [29].

For the investigation, the premix fuel line has been fed only with natural gas, while hydrogen injection has been tested on the pilot line, which is normally fuelled with natural gas. In certain conditions, in order to respect the upper limit on the hydrogen fuel fraction required to keep high CO_2 concentration, a blend of the two fuels has been made on the pilot line.

EXPERIMENTAL METHODS AND OPERATING CONDITIONS

Experimental techniques

Particle Image Velocimetry PIV measurements were performed with Dantec-Dynamics PIV system, using ©Dantec-FlowManager software for image acquisition and post processing. A Nd:YAG pulsed laser with $\lambda = 527nm$, (Litron LDY303) was employed to illuminate the central section of the liner, at the burner symmetry plane. TiO_2 particles (submicron mean size) were used to seed the air flow directly upstream of the burner, using the Lavision Particle Blaster 110 and a customed particle injector. Images were acquired with a Phantom MIRO M340 camera, coupled with a Micro NIKKOR 60mm $f/2.8$ lens and a band-pass filter ($\lambda = 527 \pm 5$) to eliminate ambient light and flame emission.

For each tested condition, about 400 pairs of images were acquired at 400 Hz with a time delay of 12 μs between the image pair. After background subtraction, adaptive grid iterative approach was applied to retrieve the velocity field. Peak validation on the image cross-correlation and the Universal Outlier Detection algorithm [32] were used to validate the vectors.

OH* chemiluminescence OH* chemiluminescence images were acquired with the same camera used for the PIV measurements, the Phantom MIRO M340, coupled with the Hamamatsu C16031-311-Ax image intensifier through a relay lens. A band-pass filter ($\lambda = 310 \pm 5$) was mounted on a Nikon UV 105mm $f/4.5$ lens to capture the OH* transition, which has its peak emission intensity at 309 nm. For the presented results the intensifier gain and gate were kept constant, with a value of 0.5 ms for the latter and an acquisition frequency of 1000 Hz.

Matlab©user-defined routines were employed for image post processing. After background subtraction and spatial calibration, the time-averaged OH* distribution is computed, in order to study the flame steady structure.

Exhaust gas analysis and other instrumentation Exhaust gas composition is measured with a HORIBA PG350 gas analyzer. The probe is plunged into the flame tube downstream of the optical liner, about 350 mm from the burner exit, to extract the exhaust gases with several radially spaced holes. A thermally insulated pipeline kept at 150°C brings the exhaust gases into a HORIBA PSS-5H refrigerator to remove water content before reaching the gas analyzer. The gas analyzer is properly calibrated right before each test employing a rack of calibrated gas mixture tanks. Emission values that will

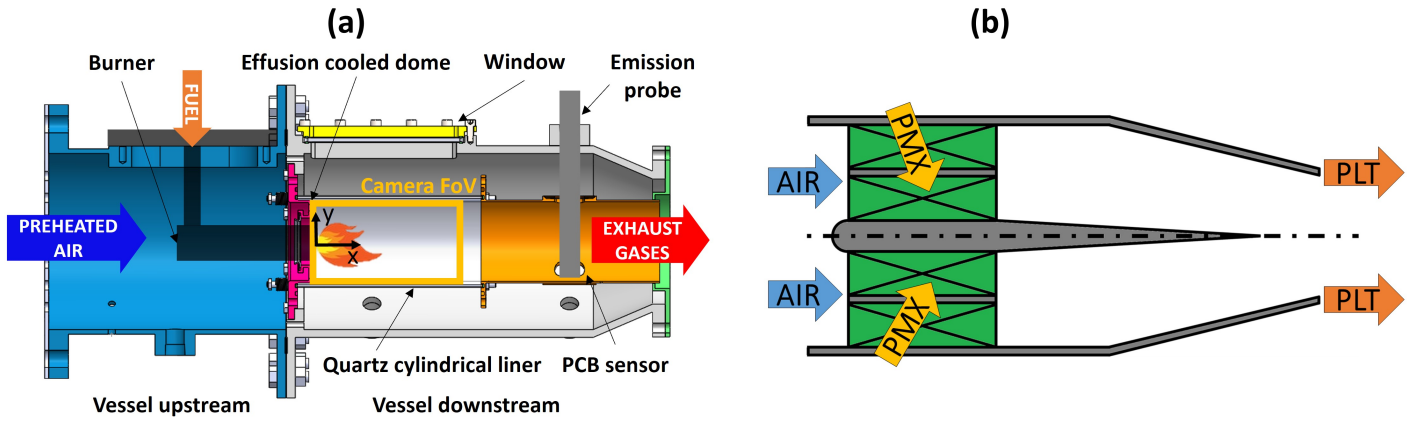

Figure 5: Cross section of the reactive test rig (a) and investigated burner schematic (b)

T_{inlet}	300	[°C]
$\Delta P/P$	4.2	[%]
TP_{total}	Constant	[kW]
PMX%	0-95	[%]
TP(H2) %	0-10	[%]
y_{O2}	23.2-15.0	[%mass]

Table 1: Tested operating conditions

be presented are CO and NO_x levels. The gas analyzer also measures O_2 and CO_2 concentration, which were monitored during tests to ensure the right operating conditions.

A high frequency (f=12.8kHz) pressure sensor (PCB) is installed on the test rig, positioned at the same axial location as the emission probe. Pressure oscillations are characterized by their Root Mean Square (RMS) value, denoted as P'_{RMS}.

Thermocouples are installed on the downstream metal duct and on the dome plate, to monitor the temperature of the components, since critical conditions may arise, particularly at the burner exit.

LabVIEW ©software is used for real-time monitoring of all the main rig parameters. The acquired data for each tested condition are averaged over 30 seconds, once steady-state conditions are reached.

Operating conditions

The experimental campaign has been performed at ambient pressure, and as explained before EGR-like conditions have been reproduced by diluting the airflow entering the test rig with CO_2. EGR condition is represented by the inlet oxygen mass fraction y_{O2}, which is a key similarity parameter between real EGR and simulated conditions.

In order to compare different operating conditions with the dual fuel configuration the total thermal power has been kept constant for all the presented results. This leads to slight differences in terms of adiabatic flame temperatures when the fuel or the oxidizer composition varies, because of the different composition of the combustion products and the resulting average specific heats of the mixture. For the investigated conditions this effect is however very limited and the resulting change in adiabatic flame temperature is practically negligible.

As explained in the burner description section, the premix fuel line has been fuelled with only natural gas, while the pilot fuel line has been fed with either hydrogen or natural gas or a blend between the two fuels. Fuel split is defined on the thermal power: PMX[%] is the thermal fraction of the premix line (always fully natural gas) over the total one, and TP(H2)[%] is the fraction of hydrogen thermal power over the burner total thermal power, which indeed comprehends both the premix and pilot contributions regardless of the type of fuel employed.

The hydrogen fraction is limited by the reduction of CO_2 content in the exhaust, and arrives up to 10% of the total thermal power.

Burner pressure drop was kept constant during the test campaign at the design value of 4.2%, adjusting the air mass flow rate, depending on the added CO_2. The inlet temperature of the oxidizer has also been kept constant at 300°C.

The tested operating conditions are reported in Table 1 and summarizing, the investigated parameters which have been varied are:

- PMX%: Premix fuel thermal power fraction
- TP(H2)%: Hydrogen thermal power fraction

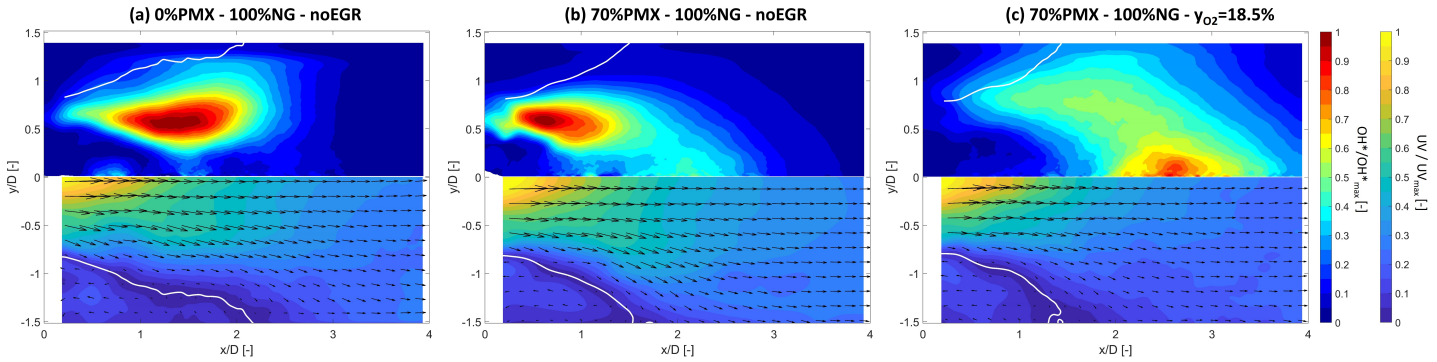

Figure 6: Inverse Abel of normalized time averaged OH* chemiluminescence images (upper half) and time averaged UV velocity magnitude (lower half) for 0%PMX (a) and 70%PMX (b) in standard conditions and 70%PMX with simulated EGR (y_{O2}=18.5%) (c). White lines correspond to UV=0 isolines

- y_{O2}: Inlet oxygen mass fraction, representing the EGR level (for standard air y_{O2}=23.2%)

To give an idea of the range of real EGR levels investigated during the test campaign, the minimum oxygen level among the presented results is around y_{O2}=15.0%. Looking at Figure 2 for the case with real EGR, this value of inlet oxygen fraction corresponds to EGR level of over 50%, for the investigated engine class (fixed CS) and adiabatic flame temperature.

RESULTS AND DISCUSSION

The baseline burner chosen for the study on operability under high EGR levels was tested both 100% fuelled with natural gas, as in conventional operation, and with hydrogen injection on the pilot line, to see any improvement in flame stability.

Burner characterization with natural gas

First of all the baseline condition is presented, with flowfield and flame structure with the burner operated with natural gas, both with pure air as oxidizer and with simulated EGR.

Camera field of view (FoV) for both PIV and OH* chemiluminescence imaging is enlightened in Figure 5b with a yellow rectangle, together with the coordinate system centered on the burner outlet. 2D PIV is able to retrieve the velocity components on the laser sheet plane (XY plane). Axial (x) and radial velocity (y) are denoted as 'U' and 'V', respectively, and 'UV' is the velocity magnitude on the XY plane. Spatial coordinates x and y have been adimesionalized with the burner exit diameter D.

Figure 6a-b shows the steady flame structure together with the velocity field measured in reactive conditions for two different fuel splits. The isoline of null velocity is reported with a white line on both PIV and OH* images, indicating the boundary of the outer recirculation zone. All the presented velocity distributions have been normalized with each own maximum in order to scale slight changes in the burner pressure drop. Inverse Abel transform of OH* images is presented in order to be congruent with PIV velocity measurements on the burner symmetry plane. By definition Abel transform assumes axialsymmetry, but in the investigated configuration pilot fuel is injected with discrete holes, and give rise to separate reaction zones near the burner exit. Therefore it is not properly correct to assume axial symmetry, but since PIV is a planar measurement, this approximation allows us to combine the information collected with the two techniques. A Fourier-based algorithm has been employed for Abel deconvolution, with the methodology described in [33].

Starting with the analysis of the mean flowfield, the typical swirl-stabilized velocity field characterized by the inner recirculation zone is missing, leaving room to a jet flame velocity field. Despite the presence of two counter rotating swirlers, the swirl number is not sufficiently high to give rise to the vortex breakdown, and the strong acceleration inside the converging duct is such that the jet remains coherent as it comes out from the burner entering the combustion chamber. The mean flowfield is very similar for the two different fuel splits of Figure 6(a)-(b), but the flame structure varies significantly. In both cases the flame stabilizes in correspondence of the outer shear layer which marks the boundary of the outer recirculation zone. The fully diffusive condition (Fig.6a-0%PMX) where the whole fuel mass flow rate is injected with the pilot jets give rise to a lifted flame, which slightly opens outward radially because of the high momentum of the pilot fuel jets.

Increasing the fraction of fuel injected with the premixed line (Fig.6b-70%PMX) the flame closes toward the centerline and comes closer to the burner exit. The shifting of the reaction zone radially towards the burner axis is due to the presence of the premixed fuel in this zone, but despite the intense mixing caused by the two counter rotating swirler, the jet peak velocity

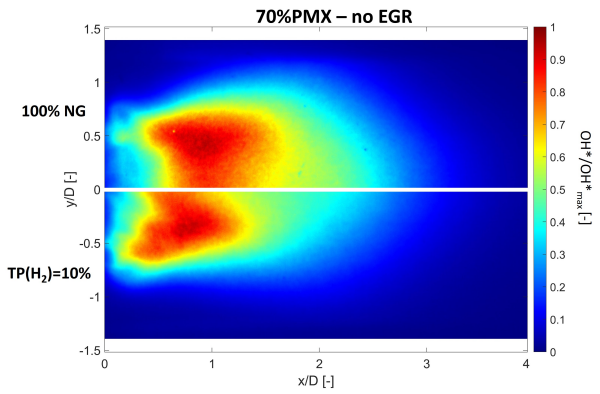

Figure 7: Time averaged OH* images (line of sight, normalized) with 70%PMX with standard air as oxidizer. Upper half: TP(H_2)=0%; Lower half: TP(H_2)=10%

at the burner exit on the centerline is too high to allow flame stabilization, and the flame is still anchored in correspondence of the pilot fuel jets and outer shear layer. Additionally, since the total fuel mass flow rate is kept constant between the two cases, the pilot jets momentum decreases and fuel jet penetration is reduced, therefore the reaction zone is less open radially toward the combustion chamber walls. A second, less intense reaction zone can be spotted on the centerline, around 2D downstream of the burner exit, where the jet diffusion lowers the airflow velocity, letting the premixed flame front stabilize. The outer recirculation zone length is reduced with higher premix split, as the thermal expansion due to the reaction zone downstream near the burner axis pushes the flow toward the combustion chamber walls.

The effect of simulated EGR on the reactive flowfield has also been investigated. Figure 6 shows the flame structure and velocity field with CO_2 addition (y_{O2}=18.5%) for 70%PMX fuel split. Looking at the upper half of the image OH* chemiluminescence shows that the reaction zone is shifted downstream and becomes more widespread for the case with CO_2 addition. On the other hand, simulated EGR does not alter significantly the flowfield, comparing the results with the case with the same fuel split and standard air as oxidizer (Fig 6b). With simulated EGR higher jet diffusion causes the velocity magnitude to decrease more rapidly moving downstream from the burner outlet, and the flow results slower near the test section exit ($x/D > 3$).

Effect of hydrogen addition with standard air as oxidizer

This section presents the effect of hydrogen addition without EGR, using standard air as oxidizer, starting with the flame steady structure studied with OH* chemiluminescence imaging.

The comparison of the reaction zone with and without hydrogen addition to the pilot fuel is presented in Figure 7. In order to have a truthful comparison both total thermal power and premixed thermal power fraction have been kept constant. When the burner is fuelled with 100% natural gas the maximum premixed fuel fraction that can be reached stably is 80%, and beyond this value strong thermoacoustic instabilities arise, as it will be detailed later. In order to show a stable condition, fuel split equal to 70%PMX has been selected, but since, as recalled before, the hydrogen thermal power fraction has to be kept under 10%, a blend of natural gas and hydrogen has been made on the pilot fuel line to reach this condition.

Despite the limited amount of hydrogen fraction in the total thermal power, the effect on the flame shape is significant, since it constitutes a large share of the thermal power on the pilot fuel, which as seen above is responsible for the flame front definition by anchoring the combustion process. The higher laminar flame speed of hydrogen takes the high reaction intensity zone closer to the burner exit, making the flame more attached. The reaction zone is overall shorter and its radial extension is also slightly reduced, because pilot fuel burns immediately at the burner exit, limiting the opening of the pilot jets. As expected the introduction of hydrogen seems to better anchor the flame near the dome, behaviour that may help stability moving toward EGR conditions. As a drawback the burner itself and the dome are subjected to higher thermal loads, given the proximity of the flame. This aspect is aggravated and can become critical in engine conditions at high pressure, even to the point of affecting the structural integrity of the burner. Nevertheless, for the tested conditions no damage has been detected on the burner outlet, and the dome temperature stayed within controlled and safe values.

One of the great advantages of doping natural gas with a small percentage of hydrogen was seen in the reduction of thermoacoustic instabilities that arise when the premix fuel fraction becomes higher than 80% when the burner is operated with natural gas.

Figure 8 shows the amplitude of pressure oscillations recorded with the dynamic pressure sensor (PCB) positioned downstream of the quartz liner, as a function of premix thermal power fraction. This time the pilot fuel line is fed 100% with hydrogen, even though the hydrogen fraction of the total thermal power is higher than 10%, in order to investigate this particular aspect, therefore the hydrogen thermal power fraction coincides with the pilot thermal power fraction.

In the case without hydrogen addition the amplitude of pressure oscillation grows suddenly and significantly as the premix fraction goes over 80%. When hydrogen is injected with the pilot fuel line, pressure oscillation amplitude starts to increase slightly around 88%, and escalates only when the premix fuel fraction is more than 90%. It is worth to point out that for the experimental campaign the burner is operated in a long tubular combustion chamber, and no diluting air is

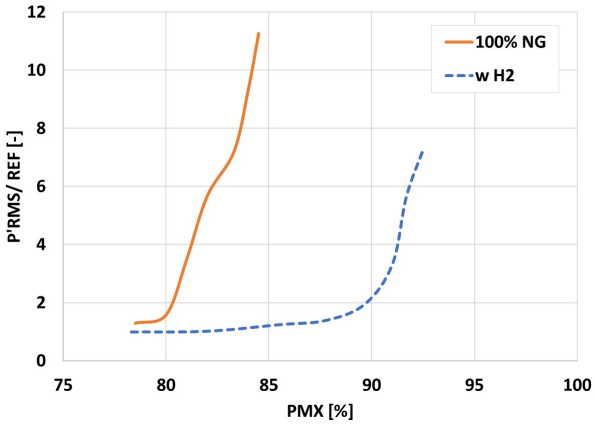

Figure 8: RMS of pressure oscillation as a function of premix thermal power split: fully natural gas (solid line) and with hydrogen (dashed line)

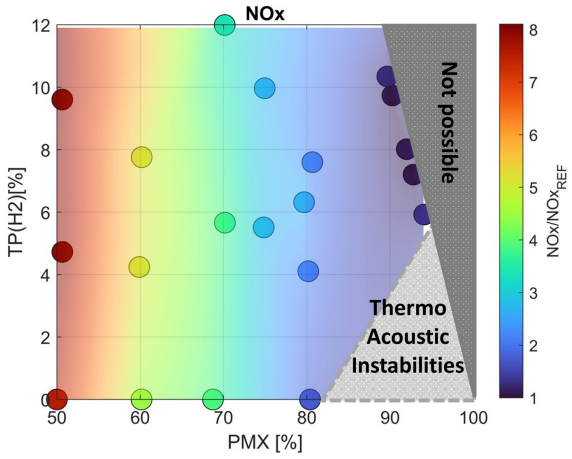

Figure 9: NO_x emission levels as a function of thermal power fraction of the premix (PMX%) and of hydrogen ($TP(H_2)$%)

injected inside: the exhaust mixes with the cooling air only at a very distant location from the burner outlet, which certainly aggravates the thermoacoustic behaviour, not helping to dampen the oscillations that arise.

These results are consistent with previous studies, as recalled in the introduction, where the beneficial role of the injection of a small amount of hydrogen to reduce instabilities has been observed in simplified configurations [17–19]. The widening of the range of stable operating conditions allows safe operation at very high premix levels, with beneficial effects on NO_x emissions, as shown in Figure 9, where NO_x are reported as a function of both premix thermal power fraction and hydrogen fraction. For the presented results a blend of hydrogen and natural gas has been prepared on the pilot line when the premix thermal power fraction is higher than 90%, otherwise pilot jets are 100% hydrogen fuelled. No hydrogen is injected with the premix line, therefore there is a "not possible" region in top right where the sum of premix split and hydrogen exceeds 100%.

Because of the wide variation in operating conditions in terms of fuel and oxidant composition, it was chosen to present emission values not corrected to a certain oxygen level, but as raw ppm measured by the gas analyzer on dry flue gas, scaled with a single reference value for all conditions, with the same approach presented in [11].

With 100% natural gas (TP(H2)=0%) NO_x level decrease linearly as the premix fuel fraction is increased, but the emergence of pressure oscillation limits this value to 80%. With hydrogen addition it is possible to obtain very low NO_x emission thanks to a higher degree of premixing, as very low values on the right upper part of the map show. With constant premix thermal power fraction, increasing the hydrogen content slightly increases NO_x levels, but the reduction that can be achieved by increasing premix is much greater than the increase due to the higher hydrogen fraction. PIV flow-fields of Figure 6, even though they were measured without hydrogen addition, suggest a very limited residence time, which helps control NO_x emissions. OH* chemiluminescence images of Figure 7 show that the reaction zone is shorter with hydrogen addition, lowering even more the residence time in high temperature zones where thermal NO_x form. This results in NO_x emissions not rising significantly even with higher hydrogen fraction. It has to be also kept in mind that this specific application with EGR and CCS strongly limits the hydrogen fraction that can be added, and the effect is consequently reduced.

Effect of hydrogen addition with simulated EGR

The previous study [20] showed how the emergence of strong thermoacoustic instabilities is one of the main factors that is limiting achievable EGR levels for the investigated burner, together with high CO emissions. The beneficial effect of hydrogen addition in reducing the amplitude of pressure fluctuations shown in the previous section has also been found in the case with simulated EGR.

Figure 10 presents the RMS of the recorded pressure oscillations as a function of the inlet oxygen content (increasing EGR going from right to left) with different fuel splits, for conditions with (dashed lines) and without (solid lines) hydrogen addition. For the baseline case without hydrogen addition, the amplitude of pressure oscillations grows as the oxygen level in the oxidizer decreases, until a certain threshold is exceeded, beyond which the oscillations decrease. Intermediate EGR ranges are therefore very problematic, and the amplitude of the oscillations increases with higher premix fuel fraction.

All the curves exhibit the same non monotonic dependence from the inlet oxygen level, with different positions and values of

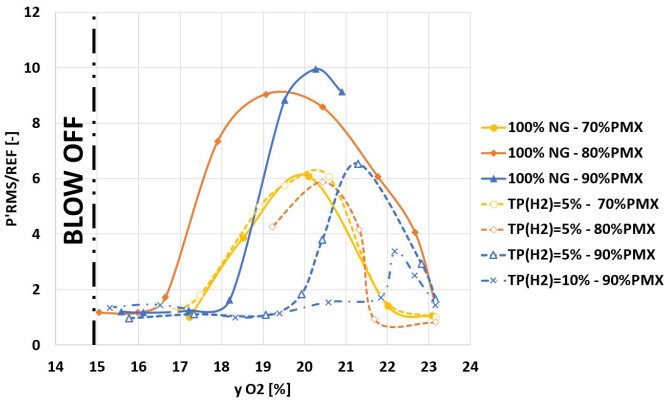

Figure 10: RMS of pressure oscillation as a function of inlet oxygen level y_{O2} with hydrogen addition (dashed lines and hollow symbols) and fully natural gas (solid lines and filled symbols) for different premixed thermal power fractions

the maximum amplitude of pressure oscillations. Instantaneous OH* images (not reported) show that during instabilities the flame is subjected to intense longitudinal fluctuations. A possible explanation of this non monotonic behaviour could be linked to the progressive elongation and lift off of the flame which happens with decreasing inlet oxygen level, as shown by chemiluminescence images of Figures 6 and 11. The modification of the flame position and length with EGR alters the coupling between heat release and pressure oscillations, which result in phase only in a certain range of inlet oxygen levels. Hydrogen addition and fuel split also affect the flame structure, therefore modifying the EGR range where constructive interference occurs and the oscillations amplitude.

In the higher pilot split case (70% PMX), the impact of the tested hydrogen content is negligible and is not sufficient to change the burner behavior, which is already more stable than under the other conditions given the substantial pilot contribution. With higher premix fuel fraction hydrogen addition significantly improves the burner behaviour: at 80%PMX maximum RMS of pressure oscillations is 40% lower with respect to the fully natural gas condition, and the threshold level over which pressure fluctuation decreases is higher, therefore enlarging the burner operating window with EGR. The gain is even higher at 90%PMX, which for the case with only natural gas was an unstable condition without EGR, as shown in the previous section. In that case (blue solid line) the effect of CO_2 addition is to dampen pressure oscillation, and the threshold oxygen level over which this happens is surprisingly higher than cases with lower premix fuel splits. At 90%PMX, with $TP(H_2)$=5% the maximum value is 40% lower than the correspondent peak without hydrogen, and if the hydrogen fraction is increased to 10% the maximum RMS value is over 70% less than the case with natural gas. In addition, and most importantly, the range of inlet oxygen levels in which the oscillations arise is very small in both cases, more narrow as the hydrogen fraction increases. The black line on the left marks the boundary with conditions in which flame completely blows off with 80%PMX without hydrogen addition, around y_{O2}=14.7%. The other operating points have similar limits, but the very high CO emissions measured at such low oxygen levels, which will be shown later in this section, do not make it worthwhile to continue the investigation in this direction.

Flame topology has been studied with OH* chemiluminescence in simulated EGR conditions with hydrogen addition. Figure 11 presents time averaged line of sight OH* images for three different inlet oxygen levels, starting with the case without simulated EGR on the left and decreasing the inlet oxygen content moving to the right. OH* intensity is normalized with the maximum of each condition to better highlight the flame structure. The upper half of the images shows the case without hydrogen addition, while for the lower half of the images hydrogen fraction of the total thermal power is kept constant at 10% with fully hydrogen fuel jets. Premix fuel split is 90% for all the presented conditions.

Starting with the results without EGR (case a, first on the left), flame shape is very different when hydrogen is injected with the pilot jets. Recalling Figure 7, where the same hydrogen fraction was injected, but with a blend with natural gas on the pilot line, when pilot jets are 100% hydrogen the variation of the flame structure is much more evident. For the case with natural gas at this highly premixed condition (Fig. 11a upper half) the reaction zone is detached from the burner exit, and a single reaction zone including both pilot and premixed fuel is visible. Pilot jets are detectable near the burner exit, but the main reaction zone is shifted downstream on the burner center-line. Compared to the case at lower premix fuel split (Fig. 7, upper half) reaction zone is more lifted and longer. For the case with hydrogen pilot jets (Fig. 11a lower half) two separate reaction zones are clearly distinguishable: hydrogen jet diffusion flames are attached at the burner exit, and the premixed natural gas burns downstream on the burner axis. A certain interaction between these two zones is present, since they are linked with an area with non-negligible OH* intensity.

When simulated EGR is introduced the fully natural gas flame becomes more and more lifted (Fig 11b-c upper half). This happens also for the reaction zone of the premixed natural gas of the case with hydrogen addition, as the downstream detached flame is shifted downstream and becomes more widespread (Fig 11b-c lower half). The highly reactive hydrogen jets instead continue to burn well attached to the burner, providing an anchor point for the reaction, but the interaction with premixed natural gas reaction zone weakens and weakens as the oxygen inlet level decreases and the distance between the two increases.

Besides thermoacoustic instabilities, the main consequence

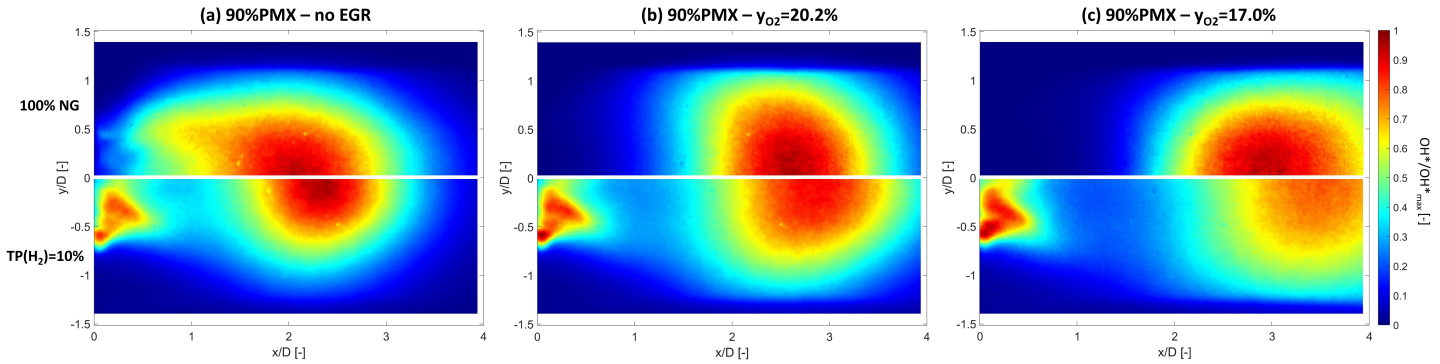

Figure 11: Time averaged OH* images (line of sight, normalized) with 90%PMX: fully natural gas (upper half) and with TP(H_2)=10% (lower half) for different inlet oxygen levels: (a) y_{O2}=23.2% (standard air), (b) y_{O2}=20.2% (c) y_{O2}=17.0%

of the lower inlet oxygen content caused by EGR, as observed in previous studies [5, 20, 34], is a sharp increase in CO emissions. Figure 12 shows CO emissions scaled with a reference value as a function of the inlet oxygen level. Cases with hydrogen addition refer to fully hydrogen pilot, and the pilot fuel split for the baseline condition with natural gas is 80%PMX. The effect of hydrogen addition is visible although not remarkable: a significant decrease of CO (about 20%) is achieved only at very low inlet oxygen content levels, probably indicating an albeit modestly improved resistance to blowout. The gain at intermediate levels is quite modest, and increasing the hydrogen fraction does not seem to have a significant effect. Recalling the OH* chemiluminescence images of Figure 11, the interaction of hydrogen jet flames with the natural gas premixed flame is not very strong even without EGR, as shown by the separation of the two reaction zones. With simulated EGR this aspect is amplified and hydrogen pilot flames are not able to substantially support the combustion of natural gas. These results suggest that a study on the pilot jets injection geometry could be a crucial aspect to be taken into account in a future optimization work.

CONCLUSIONS

The present work is aimed at studying the effect of the injection of a limited amount of hydrogen on the pilot fuel line of an industrial burner, with the purpose of increasing the resistance to high EGR levels. For the experiments EGR has been reproduced by adding CO_2 in the combustion air, which has been proven to be a precautionary approach by a dedicated chemical kinetics study.

Hydrogen addition alters the flame shape, with different extent depending on whether the same amount of hydrogen is injected pure on the pilot jets or blended with natural gas. Pure hydrogen pilot flames burn very attached to the burner outlet, but no damages or alterations were detected on the burner outlet lip. When the burner is operated with very low piloting fraction, a marked separation occurs between the hydrogen reaction zone and the natural gas one, with increasing distance as the inlet oxygen level decreases. This restrained interaction limits the reduction of CO emission that can be achieved with hydrogen addition, which is one of the main targets in the perspective of working with high EGR levels for CCS coupling.

The dynamic behaviour of the flame is found to be improved by the addition of hydrogen, both with standard air in terms of higher stably achievable premix fuel fraction, and with simulated EGR with lower pressure oscillation amplitude and increased EGR window of operability. The benefits observed in the present study in terms of low NO_x emissions with high premixing make this condition seem very interesting without EGR. Past results [20], on the other hand showed that under EGR conditions NO_x emissions decrease significantly, and the very low values are not even strongly affected by premix fraction, as the reaction zone becomes widespread, moving toward a regime of diffuse combustion. The possibility of varying the premix fraction over a wide range becomes crucial under partial load and engine regulation conditions, even more when operating under challenging conditions such as EGR.

Overall, the significant improvement in burner behaviour in terms of lower pressure fluctuations, together with the reduction, although not substantial, in CO emissions, suggest that hydrogen addition has positive implications and could be promising for expanding the operating limits of the burner under EGR conditions. In this sense pilot fuel injection mode has to be improved for the dual gas configuration in order to enhance the interaction between pilot and premixed flame fronts.

The present study highlighted the performance parameters to be taken into consideration with the perspective of optimizing the burner to work under high recirculation rates. The next step is to define an objective function that weighs these parameters in order to compare different solutions and find an optimal trade-off. Under normal conditions NO_x levels are the main target, but

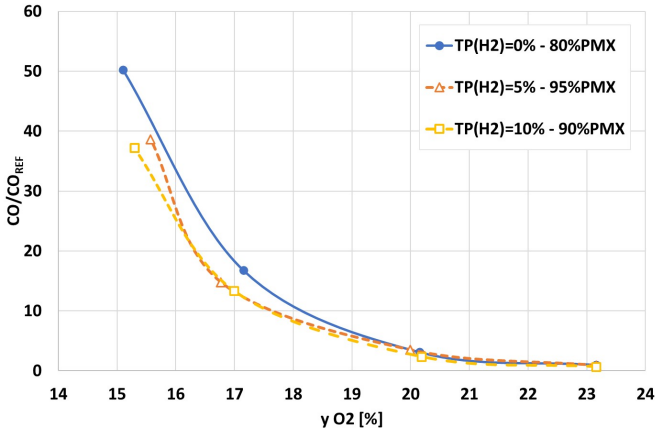

Figure 12: CO emissions with simulated EGR as a function of inlet oxygen level y_{O2}

in this particular application with EGR and CCS coupling they have a reduced impact, since they already lowered by EGR. The driving constraint is indeed the reduction of unburned emission associated with the incipient LBO, to be coupled with a wide operating range in terms of thermoacoustic instabilities.

Although these results were obtained at ambient pressure, they highlighted very important aspects to be considered during a possible re-design of a burner to work specifically under these unusual conditions. Enhanced interaction between natural gas reaction zone and hydrogen pilot flames could certainly help in this regard, and indeed fuel injection mode will be optimized.

ACKNOWLEDGMENTS

This project is funded by European Union's Horizon Europe Research and Innovation program (G.A. No 101069665)

Funded by the European Union. Views and opinions expressed are however those of the author(s) only and do not necessarily reflect those of the European Union. Neither the European Union nor the granting authority can be held responsible for them.

References

[1] IEA, 2022. World Energy Outlook 2022. Tech. rep., IEA, Paris, France.

[2] Li, H., Ditaranto, M., and Berstad, D., 2011. "Technologies for increasing CO2 concentration in exhaust gas from natural gas-fired power production with post-combustion, amine-based CO2 capture". *Energy,* ***36***(2), pp. 1124–1133.

[3] Burnes, D., Saxena, P., and Dunn, P., 2020. "Study of Using Exhaust Gas Recirculation on a Gas Turbine for Carbon Capture". p. V005T06A034.

[4] Lieuwen, T., Chang, M., and Amato, A., 2013. "Stationary gas turbine combustion: Technology needs and policy considerations". *Combustion and Flame,* ***160***(8), aug, pp. 1311–1314.

[5] Elkady, A. M., Evulet, A., Brand, A., Ursin, T. P., and Lynghjem, A., 2008. "Exhaust Gas Recirculation in DLN F-Class Gas Turbines for Post-Combustion CO2 Capture". pp. 847–854.

[6] Li, H., Elkady, A., and Evulet, A., 2009. "Effect of exhaust gas recirculation on nox formation in premixed combustion system".

[7] Halter, F., Foucher, F., Landry, L., and Mounaïm-Rousselle, C., 2009. "Effect of dilution by nitrogen and/or carbon dioxide on methane and iso-octane air flames". *Combustion Science and Technology,* ***181***, 06, pp. 813–827.

[8] Chan, Y., Zhu, M., Zhang, Z., Liu, P., and Zhang, D., 2015. "The Effect of CO2 Dilution on the Laminar Burning Velocity of Premixed Methane/Air Flames". *Energy Procedia,* ***75***, pp. 3048–3053. Clean, Efficient and Affordable Energy for a Sustainable Future: The 7th International Conference on Applied Energy (ICAE2015).

[9] Duva, B. C., Chance, L. E., and Toulson, E., 2020. "Dilution effect of different combustion residuals on laminar burning velocities and burned gas Markstein lengths of premixed methane/air mixtures at elevated temperature". *Fuel,* ***267***, p. 117153.

[10] Xie, M., Fu, J., Zhang, Y., Shu, J., Ma, Y., Liu, J., and Zeng, D., 2020. "Numerical analysis on the effects of CO2 dilution on the laminar burning velocity of premixed methane/air flame with elevated initial temperature and pressure". *Fuel,* ***264***, p. 116858.

[11] Burdet, A., Lachaux, T., de la Cruz Garcia, M., and Winkler, D., 2010. "Combustion Under Flue Gas Recirculation Conditions in a Gas Turbine Lean Premix Burner". Vol. Volume 2: Combustion, Fuels and Emissions, Parts A and B of *Turbo Expo: Power for Land, Sea, and Air*, pp. 1083–1091.

[12] Guethe, F., Stankovic, D., Genin, F., Syed, K., and Winkler, D., 2011. "Flue Gas Recirculation of the Alstom Sequential Gas Turbine Combustor Tested at High Pressure". Vol. Volume 2: Combustion, Fuels and Emissions, Parts A and B of *Turbo Expo: Power for Land, Sea, and Air*, pp. 399–408.

[13] Evulet, A. T., Elkady, A. M., Branda, A. R., and Chinn, D., 2009. "On the performance and operability of GE's dry low NOx combustors utilizing exhaust gas recirculation for post-combustion carbon capture". p. p. 3809–3816.

[14] Babazzi, G., Giannini, N., Meloni, R., Nassini, P. C., Lemmi, G., , and Andreini, A., 2023. "On the impact of the EGR on to the operability of a heavy-duty GT

combustor: a CFD investigation,". *Proc. of the 11th European Combustion Meeting, Rouen, France*.

[15] Rodriguez Camacho, J., Akiki, M., Blust, J., and O'Connor, J., 2024. "Effect of Inert Species on the Static and Dynamic Stability of a Piloted, Swirl-Stabilized Flame". *Journal of Engineering for Gas Turbines and Power,* ***146***(6), 01, p. 061021.

[16] Cheng, R., Littlejohn, D., Strakey, P., and Sidwell, T., 2008. "Laboratory investigations of a low-swirl injector with h2 and ch4 at gas turbine conditions". *Proceedings of the Combustion Institute,* ***32***, 03, pp. 3001–3009.

[17] Anderson, D. N., 1975. "Effect of hydrogen injection stability and emissions of an experimental premixed prevaporized propane burner".

[18] Oztarlik, G., Selle, L., Poinsot, T., and Schuller, T., 2020. "Suppression of instabilities of swirled premixed flames with minimal secondary hydrogen injection". *Combustion and Flame,* ***214***, Apr., pp. 266–276.

[19] Barbosa, S., de La Cruz Garcia, M., Ducruix, S., Labegorre, B., and Lacas, F., 2007. "Control of combustion instabilities by local injection of hydrogen". *Proceedings of the Combustion Institute,* ***31***(2), pp. 3207–3214.

[20] Galeotti, S., Picchi, A., Becchi, R., Meloni, R., Babazzi, G., Romano, C., and Andreini, A. "Experimental characterization of an industrial burner operated with simulated EGR". *Under review for Applied Thermal Engineering*.

[21] Wilberforce, T., Olabi, A., Sayed, E. T., Elsaid, K., and Abdelkareem, M. A., 2021. "Progress in carbon capture technologies". *Science of The Total Environment,* ***761***, p. 143203.

[22] Goodwin, D. G., Moffat, H. K., Schoegl, I., Speth, R. L., and Weber, B. W., 2023. Cantera: An object-oriented software toolkit for chemical kinetics, thermodynamics, and transport processes. `https://www.cantera.org`. Version 2.5.1.

[23] Cerutti, M., Roma, M., Picchi, A., Becchi, R., and Facchini, B., 2019. "Improving Emission and Blow-Out Characteristics of Novel Natural Gas Low NOx Burners for Heavy Duty Gas Turbine". p. V04BT04A015.

[24] Cerutti, M., Riccio, G., Andreini, A., Becchi, R., Facchini, B., and Picchi, A., 2018. "Experimental and Numerical Investigations of Novel Natural Gas Low NOx Burners for Heavy Duty Gas Turbine". p. V04BT04A031.

[25] Kline, S., and McClintock, F. A., 1953. "Describing Uncertainties in Single-Sample Experiments". *Mechanical Engineering,* ***75***, pp. 3–8.

[26] Babazzi, G., 2022. "Experimental investigation of novel gas turbine combustor concepts operating with co2 vitiated air". PhD thesis, Universià degli Studi di Firenze.

[27] Joshi, N. D., Epstein, M. J., Durlak, S., Marakovits, S., and Sabla, P. E., 1994. "Development of a Fuel Air Premixer for Aero-Derivative Dry Low Emissions Combustors". Vol. Volume 3: Coal, Biomass and Alternative Fuels; Combustion and Fuels; Oil and Gas Applications; Cycle Innovations of *Turbo Expo: Power for Land, Sea, and Air*, p. V003T06A011.

[28] Cerutti, M., Giannini, N., Ceccherini, G., Meloni, R., Matoni, E., Romano, C., and Riccio, G., 2018. "Dry Low NOx Emissions Operability Enhancement of a Heavy-Duty Gas Turbine by Means of Fuel Burner Design Development and Testing". p. V04BT04A029.

[29] Andreini, A., Facchini, B., Innocenti, A., and Cerutti, M., 2014. "Numerical analysis of a low nox partially premixed burner for industrial gas turbine applications". *Energy Procedia,* ***45***, 12, pp. 1382–1391.

[30] Innocenti, A., Andreini, A., Giusti, A., Facchini, B., Cerutti, M., Ceccherini, G., and Riccio, G., 2014. "Numerical Investigations of NOx Emissions of a Partially Premixed Burner for Natural Gas Operations in Industrial Gas Turbine". p. V04BT04A045.

[31] Innocenti, A., Andreini, A., Facchini, B., Cerutti, M., Ceccherini, G., and Riccio, G., 2015. "Design Improvement Survey for NOx Emissions Reduction of a Heavy-Duty Gas Turbine Partially Premixed Fuel Nozzle Operating With Natural Gas: Numerical Assessment". *Journal of Engineering for Gas Turbines and Power,* ***138***(1), 08, p. 011501.

[32] Dantec Dynamics, 2000. *FlowManager software and Introduction to PIV Instrumentation*.

[33] Pretzier, G., 1991. "A new method for numerical abel-inversion". *Zeitschrift für Naturforschung A,* ***46***(7), pp. 639–641.

[34] Babazzi, G., Galeotti, S., Picchi, A., Becchi, R., Cerutti, M., and Andreini, A., 2024. "Combustion Diagnostics and Emissions Measurements of a Novel Low NOx Burner for Industrial Gas Turbine Operated With CO2 Diluted Methane/Air Mixtures". *Journal of Engineering for Gas Turbines and Power,* ***146***(7), 02, p. 071007.